A silicon-rhodamine chemical-genetic hybrid for far red voltage imaging from defined neurons in brain slice

Gloria Ortiz,[‡] Pei Liu,[‡] Parker E. Deal,[‡] Ashley K. Nensel,[‡] Kayli N. Martinez,[‡] Kiarash Shamardani,[§] Hillel Adesnik,[§†] and Evan W. Miller[‡§†*]

Departments of [‡]Chemistry and [§]Molecular & Cell Biology and [†]Helen Wills Neuroscience Institute. University of California, Berkeley, California 94720, United States.

Supporting Information Placeholder

ABSTRACT: We describe the design, synthesis, and application of voltage-sensitive silicon rhodamines. Based on the Berkeley Red Sensor of Transmembrane potential, or BeRST, scaffold, the new dyes possess an isomeric molecular wire for improved alignment in the plasma membrane and contain 2' carboxylic acids for ready functionalization. Conjugation with secondary amines affords tertiary amides that localize to cellular membranes and respond to voltage changes with a 24% ΔF/F per 100 mV. When combined with a flexible polyethyleneglycol (PEG) linker and a chloroalkane HaloTag ligand, the new indicators, or isoBeRST dyes, enable voltage imaging from genetically defined cells and neurons. Covalent ligation of isoBeRST to cell surface-expressed HaloTag enzymes provides up to 3-fold improved labeling over previous, rhodamine-based hybrid strategies. We show that isoBeRST-Halo hybrid indicators achieve single-trial voltage imaging of membrane potential dynamics from dissociated rat hippocampal neurons or mouse cortical neurons in brain slices. With far-red/near infrared excitation and emission, turn-on response to action potentials, effective cell labeling in thick tissue, and excellent photostability, the new isoBeRST-Halo derivatives provide an important complement to voltage imaging in neurobiology.

Voltage imaging in the central nervous system promises to transform the ways in which we observe brain systems.[1-2] Recently, a number of approaches to voltage imaging have emerged, including methods that rely solely on synthetic dyes[3-9] or genetically encoded proteins.[10-17] Alternatively, hybrid methodologies can combine the unique properties of synthetic dyes—high molecular brightness, wide availability of colors, or fast response kinetics—with the cellular specificity of genetically encoded methods.[18-23] Our group recently reported the development of a completely synthetic voltage-sensitive fluorophore, Berkeley Red Sensor of Transmembrane potential 1, or BeRST 1, a silicon-rhodamine-based indicator that we hypothesize operates via voltage-sensitive photoinduced electron transfer (PeT).[24] The high sensitivity (24% ΔF/F per 100 mV), fast response kinetics, photostability, and far red/near infra-red excitation and emission profile have enabled the use of BeRST 1 in a number of voltage imaging applications.[25-31]

Scheme 1. Overview of isoBeRST-Halo

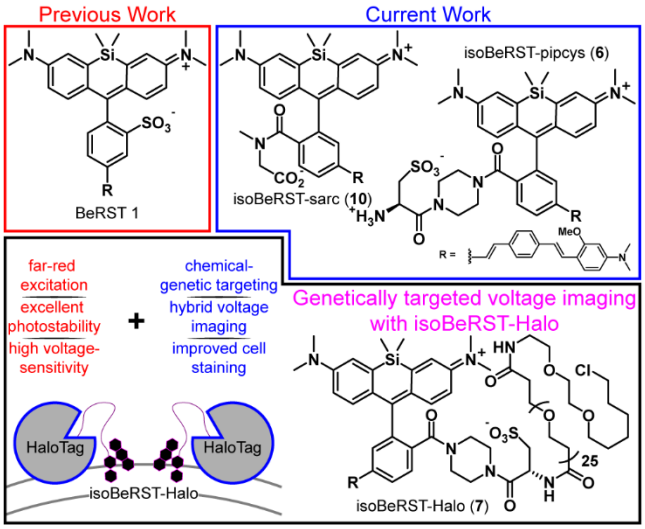

However, the use of BeRST 1 has been largely restricted to *in vitro* systems of homogeneous cell types. Usage in more complex settings, like thick brain tissue, remains a challenge because of a lack of methods to genetically target BeRST 1 to defined cells. Here we report two new synthetic BeRST dyes and show that this new class of indicator can be combined with a genetically-encoded protein tether to enable voltage imaging from defined cells in mouse brain slice.

To enable genetic targeting of BeRST-style dyes, we redesigned the synthesis of BeRST. We replaced the 2'-sulfonate of BeRST with a carboxylate: this allows for addition of covalent tethers and mimics our previous design success with Rhodamine-based Voltage Reporters (RhoVRs).[32-33] We also used the 5' version of molecular wire, since the 5', or isomeric, version showed improved voltage sensitivity compared to the 4' RhoVR.[32] Additionally, the commercial availability of the precursors to the aldehyde starting material substantially simplified the synthetic route (**Scheme S1**). The optimized synthesis of isoBeRST-sarc **10** begins with a Heck reaction between fluorophore **1**[34-35] and (*E*)-3-methoxy-*N*,*N*-dimethyl-4-(4-vinylstyryl)aniline[36] to obtain carboxy silicon rhodamine **8** (**Scheme S1**). Dye **8** is coupled to sarcosine *tert*-butyl ester using oxalyl chloride, followed

Scheme 2. Synthesis of isoBeRST-pipcys (6) and isoBeRST-Halo (7)

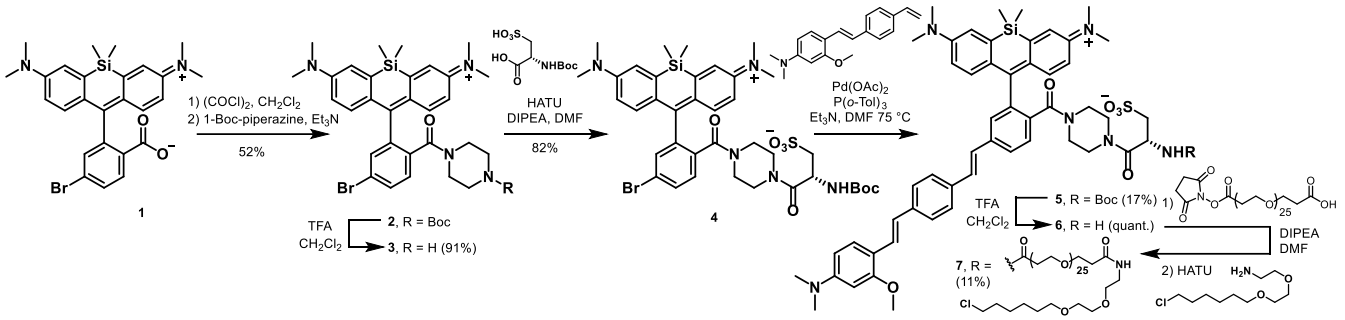

Table 1. Properties of isoBeRST indicators

Compound	λ_{max} / nm[a]	λ_{em} / nm[a]	ε	Φ[a,b]	% ΔF/F / 100 mV[c]	Relative brightness[d]
isoBeRST-pipcys **6**	662	681	172,000	0.061	24 ± 1.9	100%
isoBeRST-Halo **7**	662	677	-	0.042	21 ± 1.2	30%
isoBeRST-sarc **10**	661	681	107,700	0.098	24 ± 2.6	-

[a]In PBS, pH 7.4, 0.1% SDS. [b]Referenced to Cy5.5-carboxylic acid in PBS. [c]Voltage-clamped HEK cells. Error is ± S.D. for n = 5-6 cells. [d]In HEK cells. Error is ± S.E.M for n = 4 coverslips (>100 cells per coverslip for relative brightness).

by a TFA-catalyzed deprotection of the *tert*-butyl ester to give the voltage-sensitive fluorophore isoBeRST-sarc **10**, which is the Si-rhodamine analog of RhoVR 1.[32]

We also synthesized the piperazine-cysteic acid conjugate of isoBeRST, or isoBeRST-pipcys **6**, since this configuration allowed us to target RhoVR dyes to specific cells using HaloTag (**Scheme 2**).[33] The synthesis of isoBeRST-pipcys **6** and isoBeRST-Halo **7** follows a sequential amide-coupling / Heck coupling sequence. This provided higher overall yields than amide coupling with the assembled molecular wire/fluorophore **8**. The cyclic, piperazine-derived tertiary amide of **3** appears more stable than the amide formed from sarcosine, based on its ability to undergo successful Pd-catalyzed synthesis of isoBeRST-pipcys **6**. The route begins with oxalyl chloride mediated coupling of reported silicon rhodamine **1** with 1-Boc-piperazine, followed by TFA deprotection to yield silicon rhodamine **2** (**Scheme 2**). A second coupling mediated by HATU installed Boc-L-cysteic acid, affording **3**. Compound **3** was then submitted to a Heck reaction with phenylene-vinylene wire. Subsequent TFA deprotection gives voltage-sensitive fluorophore isoBeRST-pipcys **6** in 17% yield. In a one-pot sequence, isoBeRST-pipcys **6** is reacted with acid-dPEG$_{25}$-NHS ester, followed by addition of HaloTag amine (**Scheme 2**) and HATU. The complete reaction was purified via preparative-scale HPLC to yield the genetically-targetable isoBeRST-Halo **7** in 11% yield.

Spectroscopic characterization of isoBeRST-sarc **10**, isoBeRST-pipcys **6**, and isoBeRST-Halo **7** reveals that all three voltage indicators possess similar photophysical properties (**Table 1, Figures 1, S1, and S2**). IsoBeRST-sarc **10** displays a λ_{max} at 661 nm, similar to BeRST 1 (λ_{max} = 658 nm) and identical to isoBeRST-pipcys **6** and isoBeRST-Halo **7**. IsoBeRST-sarc **10** possesses an emission maximum of 681 nm and a quantum yield (Φ) of 9.8%, while isoBeRST-pipcys **6** has an emission maximum of 681 nm and Φ of 6.1%. IsoBeRST-Halo **7** has an emission maximum of 677 nm and Φ of 4.2%.

All of the new Si-rhodamine indicators are voltage-sensitive. In human embryonic kidney (HEK) cells untargeted dyes isoBeRST-sarc **10** (**Figure S1**) and isoBeRST-pipcys **6** (**Figure S2**) localize to the plasma membrane and are voltage sensitive. IsoBeRST-pipcys **6** has a voltage sensitivity of 24% ± 2% ΔF/F per 100 mV (SNR = 110 ± 15), identical to BeRST 1 (24% ± 5% ΔF/F per 100 mV)[24] and to isoBeRST-sarc **10** (**Table 1**). We selected isoBeRST-pipcys **6** to evaluate in neurons because of the higher yielding synthesis and stability compared to isoBeRST-sarc **10**. In cultured rat hippocampal neurons, isoBeRST-pipcys **6** (500 nM) provided clear resolution of action potentials (**Figure S3**).

The genetically-targetable isoBeRST-Halo **7** selectively labels HEK cells expressing cell-surface HaloTag (**Figure 1 and S4**). We expressed HaloTag on the surface of mammalian cells using a fusion with a single-pass transmembrane domain.[33] At 500 nM isoBeRST-Halo **7**, cells expressing cell-surface HaloTag are approximately 14-fold brighter than un-transfected control cells (**Figure S4f**). At lower concentrations (50 nM), fluorescence intensity in HaloTag-expressing cells increases to approximately 30-fold over non-HaloTag expressing cells (**Figure S4f**). This is three times better contrast than RhoVR-Halo labeling (10-15 fold).[33] Although expression levels of HaloTag vary slightly with transient transfection, a screen of isoBeRST-Halo **7** concentrations reveals that HaloTag binding sites appear to saturate at around 50 to 100 nM (**Figure S4f**). The drop in contrast ratio, from ~30-fold at 50 nM to about 14-fold at 500 nM comes from a small increase in background staining in control cells (an increase of about 4 percentage points, from 5% to 9%). Importantly, isoBeRST **7** (50 nM) is voltage-sensitive, with a voltage sensitivity of 21% ± 1% ΔF/F per 100 mV and an SNR of 42 ± 7 (**Figure 1** and **Table 1**). IsoBeRST-Halo **7** maintains about the same voltage sensitivity as isoBeRST-pipcys **6** (500 nM), indicating that the covalently tethered dye remains properly oriented in the plasma membrane (**Table 1** and **Figure 1**).

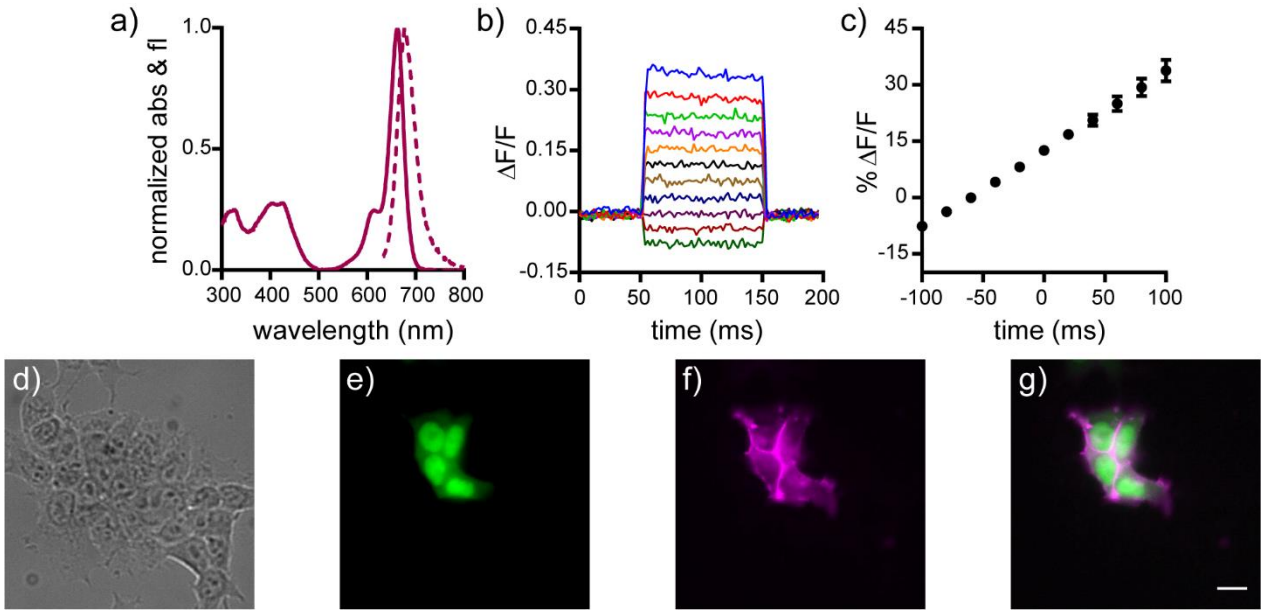

Figure 1. Cellular and *in vitro* characterization of isoBeRST-Halo **7**. **a)** Normalized absorbance (solid line) and emission (dashed line) spectra of isoBeRST-Halo **7** in PBS, pH 7.4. **b)** Plot of the fractional change in fluorescence of **7** vs time for 100 ms hyper- and depolarizing steps (±100 mV in 20 mV increments) from a holding potential of -60 mV for single HEK cells under whole-cell voltage-clamp mode. **c)** Plot of % ΔF/F vs final membrane potential. Data are mean ±S.D. for n = 6 cells. **d-g)** Wide-field microscopy images of HEK cells transfected with CMV-HaloTag-pDisplay and stained with isoBeRST-Halo **7** (50 nM, 30 mins). **d)** DIC image of HEK cells. **e)** Nuclear EGFP fluorescence indicates HaloTag expression. **f)** isoBeRST-Halo fluorescence. **g)** Merge of fluorescence from EGFP (green) and isoBeRST-Halo (magenta). Scale bar is 10 μm.

Covalently-tethered isoBeRST-Halo **7** visualizes voltage changes in genetically-defined neurons. Dissociated, cultured rat hippocampal neurons transfected with HaloTag under control of the synapsin promotor (to drive neuron-specific expression) were labeled with 50 nM isoBeRST-Halo. Neurons expressing HaloTag show excellent selectivity, revealing good localization of the dye to the outer membrane (**Figure 2 and S5**). The best contrast between HaloTag-expressing and control cells is achieved using 50 nM isoBeRST-Halo (50x brighter than untransfected cells) when compared to 100 nM isoBeRST-Halo (30x brighter than untransfected cells). High isoBeRST-Halo fluorescence correlates with high levels of HaloTag/GFP (**Figure S5e-g**). Using these optimized loading conditions, we demonstrated the ability to record spontaneous and evoked activity in neurons (**Figure 2e** and **Figure S6**). IsoBeRST-Halo responded to field stimulated evoked action potentials with a 10% ± 0.3% ΔF/F and SNR of 15 ± 1 (19 cells).

We next evaluated the ability of isoBeRST-Halo **7** to monitor voltage dynamics from neurons in brain slice. We introduced genes for HaloTag and a co-expression marker, blue fluorescent protein, or BFP, on separate plasmids via *in utero* electroporation in mouse embryos.[37] We prepared tissue slices from the brains of these mice and stained the slices with isoBeRST-Halo **7** (250 to 500 nM, 15 min). Confocal fluorescence microscopy reveals localization of isoBeRST-Halo fluorescence in the cell membranes of neurons that express BFP and HaloTag (**Figure 3a,b**). Both cell bodies and more distal processes like axonal and dendritic membranes appear fluorescent (**Figure 3a,b** and **Figure S7**), mirroring results in dissociated rat neurons (**Figure 2**). Unlabeled

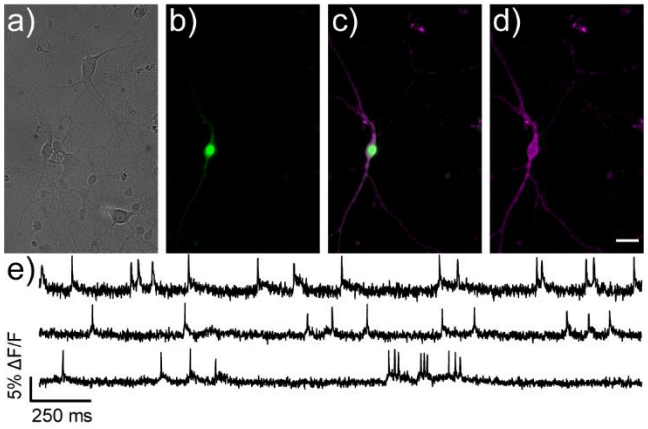

Figure 2. Monitoring spontaneous activity in neurons with isoBeRST-Halo **7**. **a-d)** Wide-field microscopy images of isoBeRST-Halo in a HaloTag-expressing neuron. **a)** DIC image of neurons. **b)** Nuclear EGFP fluorescence indicates HaloTag expression. **c)** Merge of EGFP (green) and isoBeRST-Halo (magenta) fluorescence. **d)** isoBeRST-Halo fluorescence is restricted to the membrane. Scale bar is 20 μm. **e)** Optical recordings at 500 Hz (1.94 W/cm²) of spontaneous activity shown as ΔF/F vs time for HaloTag-expressing neurons from different coverslips labeled with **7**.

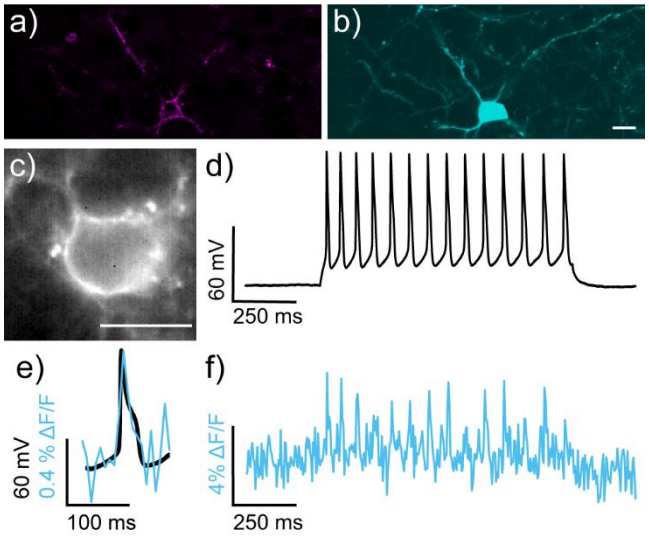

Figure 3. Characterization of isoBeRST-Halo in mouse brain slice expressing HaloTag-pDisplay and pCAG-BFP. **a-b)** Confocal microscopy images of a HaloTag-expressing neuron stained with **a)** isoBeRST-Halo (500 nM, 30 min, 23 °C) and expressing **b)** BFP. Scale bar is 20 μm. **c)** Wide-field microscopy image of isoBeRST-Halo stained slice acquired during patch-clamp electrophysiology. **d)** Plot of voltage vs. time for cell in panel (**c**). **e)** Overlay of membrane potential (black) and isoBeRST-Halo fluorescence (teal). **f)** Plot of ΔF/F fluorescence from isoBeRST-Halo fluorescence for the cell in panel (**c**). The ΔF/F trace was acquired at 0.5 kHz and represents single-trial acquisition.

cell bodies appear as dark spots, indicating that labeling of neurons requires HaloTag expression (**Figure S7**). In mouse brain slices, isoBeRST-Halo is voltage-sensitive. Simultaneous patch clamp electrophysiology and fluorescence imaging establishes that isoBeRST-Halo tracks action potentials in a single trial (**Figure 3c-f**). The voltage-sensitive fluorescence of isoBeRST-Halo corresponds well with the electrode-based recording of action potentials (**Figure 3e**). IsoBeRST-Halo **7** detects action potentials (**Figure 3f**) with a SNR of 4.9 ± 1.3 (S.D., n = 10 spikes) and a ΔF/F of 3.3% ± 0.6% (S.D., n = 10 spikes). The sensitivity of isoBeRST-Halo **7** in brain slices compares favorably to RhoVR-Halo, which has a higher voltage sensitivity (34%) than isoBeRST-Halo (21%) in HEK cells and has an SNR of 3.3 and a ΔF/F of 4.3% in brain slice.[33]

In summary, we describe the design, synthesis, and application of a new silicon-rhodamine-based voltage-sensitive fluorophores. The new BeRST derivatives rely on a 2' carboxylate, rather than sulfonate, and can be combined with secondary amines to generate tertiary amides that function well as voltage indicators in their own right, with ΔF/F values matching the sulfonated-based BeRST 1.[24] Unlike BeRST 1, however, the new carboxy-containing isoBeRST derivatives reported here can be readily incorporated into a hybrid genetic targeting framework. When combined in this way, isoBeRST-Halo (**7**) enables selective labeling of cells expressing cell-surface HaloTag, including HEK293T cells, dissociated rat hippocampal neurons, and cortical neurons in mouse brain slices. Labeling with isoBeRST-Halo provides improved contrast between HaloTag-expressing and non-expressing cells, compared to RhoVR1-Halo.[33] In all of these contexts, isoBeRST-Halo is voltage-sensitive, with ΔF/F values comparable to the parent BeRST 1 indicator.

Voltage imaging with isoBeRST-Halo (**7**) provides an important complement to voltage imaging efforts. It offers a turn-on indicator for action potentials, possesses an excitation spectrum aligned with common excitation sources, operates in the far-red / near infrared, and takes advantage of the high photostability of silicon-rhodamines.[24] In the future, we will maximize expression of cell-surface HaloTag, since one limitation of the covalent tethering approach is that the stoichiometric labeling limits the number of indicators that can be added to a cell membrane. Finally, we envision that isoBeRST-Halo can pair with optically[33] and enzymatically orthogonal hybrid genetic labeling strategies[38-40] to provide multi-color voltage imaging in complex tissues.

Supporting Information

Supplementary data, including supporting figures, spectra, procedures, and analysis. This material is available free of charge via the Internet at http://pubs.acs.org.

Corresponding Author

* Evan W. Miller, evanwmiller@berkeley.edu

ACKNOWLEDGMENT

Research in the Miller lab is supported by grants from the NIH (R01NS098088) and Klingenstein-Simon Foundations (40746). E.W.M and H.A. acknowledge support from NSF Neuronex (1707350). G.O. was supported by a Gilliam Research Fellowship from Howard Hughes Medical Institute. P.L. was supported by a graduate fellowship from A*STAR. K.N.M. was supported in part by a training grant from the NIH (T32GM066698). Confocal imaging experiments were performed at the CRL Molecular Imaging Center, supported by the Helen Wills Neuroscience Institute. HRMS data were collected at the QB3/Chemistry Mass Spectrometry Facility (UC Berkeley) with the assistance of Dr. Ulla N. Andersen.

REFERENCES

1. Peterka, D. S.; Takahashi, H.; Yuste, R., Imaging Voltage in Neurons. *Neuron* **2011,** *69* (1), 9-21.
2. Scanziani, M.; Häusser, M., Electrophysiology in the age of light. *Nature* **2009,** *461* (7266), 930-939.
3. Liu, P.; Miller, E. W., Electrophysiology, Unplugged: Imaging Membrane Potential with Fluorescent Indicators. *Accounts of Chemical Research* **2020,** 53 (1), 11-19.
4. Sayresmith, N. A.; Saminathan, A.; Sailer, J. K.; Patberg, S. M.; Sandor, K.; Krishnan, Y.; Walter, M. G., Photostable Voltage-Sensitive Dyes Based on Simple, Solvatofluorochromic, Asymmetric Thiazolothiazoles. *Journal of the American Chemical Society* **2019,** *141* (47), 18780-18790.
5. Reeve, J. E.; Corbett, A. D.; Boczarow, I.; Kaluza, W.; Barford, W.; Bayley, H.; Wilson, T.; Anderson, H. L., Porphyrins for Probing Electrical Potential Across Lipid Bilayer Membranes by Second Harmonic Generation. *Angewandte Chemie International Edition* **2013,** 52 (34), 9044-9048.
6. Rowland, C. E.; Susumu, K.; Stewart, M. H.; Oh, E.; Mäkinen, A. J.; O'Shaughnessy, T. J.; Kushto, G.; Wolak, M. A.; Erickson, J. S.; L. Efros, A.; Huston, A. L.; Delehanty, J. B., Electric Field Modulation of Semiconductor Quantum Dot Photoluminescence: Insights Into the Design of Robust Voltage-Sensitive Cellular Imaging Probes. *Nano Letters* **2015,** *15* (10), 6848-6854.
7. Yan, P.; Acker, C. D.; Zhou, W. L.; Lee, P.; Bollensdorff, C.; Negrean, A.; Lotti, J.; Sacconi, L.; Antic, S. D.; Kohl, P.; Mansvelder, H. D.; Pavone, F. S.; Loew, L. M., Palette of fluorinated voltage-sensitive hemicyanine dyes. *Proceedings of the National Academy of Sciences of the United States of America* **2012,** *109* (50), 20443-8.
8. Miller, E. W.; Lin, J. Y.; Frady, E. P.; Steinbach, P. A.; Kristan, W. B.; Tsien, R. Y., Optically monitoring voltage in neurons by photo-

induced electron transfer through molecular wires. *Proceedings of the National Academy of Sciences* **2012,** *109* (6), 2114-2119.

9. Treger, J. S.; Priest, M. F.; Iezzi, R.; Bezanilla, F., Real-time imaging of electrical signals with an infrared FDA-approved dye. *Biophysical journal* **2014,** *107* (6), Lo9-12.

10. Piatkevich, K. D.; Jung, E. E.; Straub, C.; Linghu, C.; Park, D.; Suk, H. J.; Hochbaum, D. R.; Goodwin, D.; Pnevmatikakis, E.; Pak, N.; Kawashima, T.; Yang, C. T.; Rhoades, J. L.; Shemesh, O.; Asano, S.; Yoon, Y. G.; Freifeld, L.; Saulnier, J. L.; Riegler, C.; Engert, F.; Hughes, T.; Drobizhev, M.; Szabo, B.; Ahrens, M. B.; Flavell, S. W.; Sabatini, B. L.; Boyden, E. S., A robotic multidimensional directed evolution approach applied to fluorescent voltage reporters. *Nature chemical biology* **2018,** *14* (4), 352-360.

11. Hochbaum, D. R.; Zhao, Y.; Farhi, S. L.; Klapoetke, N.; Werley, C. A.; Kapoor, V.; Zou, P.; Kralj, J. M.; Maclaurin, D.; Smedemark-Margulies, N.; Saulnier, J. L.; Boulting, G. L.; Straub, C.; Cho, Y. K.; Melkonian, M.; Wong, G. K.; Harrison, D. J.; Murthy, V. N.; Sabatini, B. L.; Boyden, E. S.; Campbell, R. E.; Cohen, A. E., All-optical electrophysiology in mammalian neurons using engineered microbial rhodopsins. *Nature methods* **2014,** *11* (8), 825-33.

12. Kannan, M.; Vasan, G.; Huang, C.; Haziza, S.; Li, J. Z.; Inan, H.; Schnitzer, M. J.; Pieribone, V. A., Fast, in vivo voltage imaging using a red fluorescent indicator. *Nature methods* **2018,** *15* (12), 1108-1116.

13. Abdelfattah, A. S.; Farhi, S. L.; Zhao, Y.; Brinks, D.; Zou, P.; Ruangkittisakul, A.; Platisa, J.; Pieribone, V. A.; Ballanyi, K.; Cohen, A. E.; Campbell, R. E., A Bright and Fast Red Fluorescent Protein Voltage Indicator That Reports Neuronal Activity in Organotypic Brain Slices. *The Journal of neuroscience : the official journal of the Society for Neuroscience* **2016,** *36* (8), 2458-72.

14. Jin, L.; Han, Z.; Platisa, J.; Wooltorton, Julian R. A.; Cohen, Lawrence B.; Pieribone, Vincent A., Single Action Potentials and Subthreshold Electrical Events Imaged in Neurons with a Fluorescent Protein Voltage Probe. *Neuron* **2012,** *75* (5), 779-785.

15. Gong, Y.; Huang, C.; Li, J. Z.; Grewe, B. F.; Zhang, Y.; Eismann, S.; Schnitzer, M. J., High-speed recording of neural spikes in awake mice and flies with a fluorescent voltage sensor. *Science (New York, N.Y.)* **2015,** *350* (6266), 1361-6.

16. Lin, M. Z.; Schnitzer, M. J., Genetically encoded indicators of neuronal activity. *Nature neuroscience* **2016,** *19* (9), 1142-53.

17. Wu, J.; Liang, Y.; Chen, S.; Hsu, C.-L.; Chavarha, M.; Evans, S. W.; Shi, D.; Lin, M. Z.; Tsia, K. K.; Ji, N., Kilohertz two-photon fluorescence microscopy imaging of neural activity in vivo. *Nature methods* **2020,** *17* (3), 287-290.

18. Chanda, B.; Blunck, R.; Faria, L. C.; Schweizer, F. E.; Mody, I.; Bezanilla, F., A hybrid approach to measuring electrical activity in genetically specified neurons. *Nature neuroscience* **2005,** *8* (11), 1619-26.

19. Ghitani, N.; Bayguinov, P. O.; Ma, Y.; Jackson, M. B., Single-trial imaging of spikes and synaptic potentials in single neurons in brain slices with genetically encoded hybrid voltage sensor. *Journal of neurophysiology* **2015,** *113* (4), 1249-59.

20. Ng, D. N.; Fromherz, P., Genetic Targeting of a Voltage-Sensitive Dye by Enzymatic Activation of Phosphonooxymethyl-ammonium Derivative. *ACS Chemical Biology* **2011,** *6* (5), 444-451.

21. Sundukova, M.; Prifti, E.; Bucci, A.; Kirillova, K.; Serrao, J.; Reymond, L.; Umebayashi, M.; Hovius, R.; Riezman, H.; Johnsson, K.; Heppenstall, P. A., A Chemogenetic Approach for the Optical Monitoring of Voltage in Neurons. *Angewandte Chemie (International ed. in English)* **2019,** *58* (8), 2341-2344.

22. Fiala, T.; Wang, J.; Dunn, M.; Šebej, P.; Choi, S. J.; Nwadibia, E. C.; Fialova, E.; Martinez, D. M.; Cheetham, C. E.; Fogle, K. J.; Palladino, M. J.; Freyberg, Z.; Sulzer, D.; Sames, D., Chemical Targeting of Voltage Sensitive Dyes to Specific Cells and Molecules in the Brain. *Journal of the American Chemical Society* **2020,** *142* (20), 9285-9301.

23. Abdelfattah, A. S.; Kawashima, T.; Singh, A.; Novak, O.; Liu, H.; Shuai, Y.; Huang, Y.-C.; Campagnola, L.; Seeman, S. C.; Yu, J.; Zheng, J.; Grimm, J. B.; Patel, R.; Friedrich, J.; Mensh, B. D.; Paninski, L.; Macklin, J. J.; Murphy, G. J.; Podgorski, K.; Lin, B.-J.; Chen, T.-W.; Turner, G. C.; Liu, Z.; Koyama, M.; Svoboda, K.; Ahrens, M. B.; Lavis, L. D.; Schreiter, E. R., Bright and photostable chemigenetic indicators for extended in vivo voltage imaging. *Science (New York, N.Y.)* **2019,** *365* (6454), 699-704.

24. Huang, Y.-L.; Walker, A. S.; Miller, E. W., A Photostable Silicon Rhodamine Platform for Optical Voltage Sensing. *Journal of the American Chemical Society* **2015,** *137* (33), 10767-10776.

25. Ginebaugh, S. P.; Cyphers, E. D.; Lanka, V.; Ortiz, G.; Miller, E. W.; Laghaei, R.; Meriney, S. D., The Frog Motor Nerve Terminal Has Very Brief Action Potentials and Three Electrical Regions Predicted to Differentially Control Transmitter Release. *Journal of Neuroscience* **2020,** *40* (18), 3504-3516.

26. Klimas, A.; Ortiz, G.; Boggess, S. C.; Miller, E. W.; Entcheva, E., Multimodal on-axis platform for all-optical electrophysiology with near-infrared probes in human stem-cell-derived cardiomyocytes. *Progress in Biophysics & Molecular Biology* **2020,** *154*, 62-70.

27. McNamara, H. M.; Dodson, S.; Huang, Y. L.; Miller, E. W.; Sandstede, B.; Cohen, A. E., Geometry-Dependent Arrhythmias in Electrically Excitable Tissues. *Cell Systems* **2018,** *7* (4), 359-+.

28. McNamara, H. M.; Salegame, R.; Al Tanoury, Z.; Xu, H. T.; Begum, S.; Ortiz, G.; Pourquie, O.; Cohen, A. E., Bioelectrical domain walls in homogeneous tissues. *Nature Physics* **2020,** *16* (3), 357-+.

29. Streit, J.; Kleinlogel, S., Dynamic all-optical drug screening on cardiac voltage-gated ion channels. *Scientific Reports* **2018,** *8*.

30. Lee-Montiel, F. T.; Laemmle, A.; Dumont, L.; Lee, C. S.; Huebsch, N.; Charwat, V.; Okochi, H.; Hancock, M. J.; Siemons, B.; Bogess, S.; Goswami, I.; Miller, E. W.; Willenbring, H.; Healy, K., Integrated hiPSC-based liver and heart microphysiological systems predict unsafe drug-drug interaction. *bioRxiv* **2020**, 2020.05.24.112771.

31. Huebsch, N.; Charrez, B.; Siemons, B.; Boggess, S. C.; Wall, S.; Charwat, V.; Jæger, K. H.; Lee Montiel, F. T.; Jeffreys, N. C.; Deveshwar, N.; Edwards, A.; Serrano, J.; Snuderl, M.; Stahl, A.; Tveito, A.; Miller, E. W.; Healy, K. E., Metabolically-Driven Maturation of hiPSC-Cell Derived Heart-on-a-Chip. *bioRxiv* **2018**, 485169.

32. Deal, P. E.; Kulkarni, R. U.; Al-Abdullatif, S. H.; Miller, E. W., Isomerically Pure Tetramethylrhodamine Voltage Reporters. *J Am Chem Soc* **2016,** *138* (29), 9085-8.

33. Deal, P. E.; Liu, P.; Al-Abdullatif, S. H.; Muller, V. R.; Shamardani, K.; Adesnik, H.; Miller, E. W., Covalently Tethered Rhodamine Voltage Reporters for High Speed Functional Imaging in Brain Tissue. *Journal of the American Chemical Society* **2020,** *142* (1), 614-622.

34. Wang, B.; Chai, X.; Zhu, W.; Wang, T.; Wu, Q., A general approach to spirolactonized Si-rhodamines. *Chemical Communications* **2014,** *50* (92), 14374-14377.

35. Kozma, E.; Estrada Girona, G.; Paci, G.; Lemke, E. A.; Kele, P., Bioorthogonal double-fluorogenic siliconrhodamine probes for intracellular super-resolution microscopy. *Chemical Communications* **2017,** *53*, 6696-6699.

36. Woodford, C. R.; Frady, E. P.; Smith, R. S.; Morey, B.; Canzi, G.; Palida, S. F.; Araneda, R. C.; Kristan, W. B.; Kubiak, C. P.; Miller, E. W.; Tsien, R. Y., Improved PeT Molecules for Optically Sensing Voltage in Neurons. *Journal of the American Chemical Society* **2015,** *137* (5), 1817-1824.

37. Tabata, H.; Nakajima, K., Efficient in utero gene transfer system to the developing mouse brain using electroporation: visualization of neuronal migration in the developing cortex. *Neuroscience* **2001,** *103* (4), 865-872.

38. Liu, P.; Grenier, V.; Hong, W.; Muller, V. R.; Miller, E. W., Fluorogenic Targeting of Voltage-Sensitive Dyes to Neurons. *Journal of the American Chemical Society* **2017,** *139* (48), 17334-17340.

39. Ortiz, G.; Liu, P.; Naing, S. H. H.; Muller, V. R.; Miller, E. W., Synthesis of Sulfonated Carbofluoresceins for Voltage Imaging. *Journal of the American Chemical Society* **2019,** *141* (16), 6631-6638.

40. Grenier, V.; Daws, B. R.; Liu, P.; Miller, E. W., Spying on Neuronal Membrane Potential with Genetically Targetable Voltage Indicators. *Journal of the American Chemical Society* **2019,** *141* (3), 1349-1358.

Authors are required to submit a graphic entry for the Table of Contents (TOC) that, in conjunction with the manuscript title, should give the reader a representative idea of one of the following: A key structure, reaction, equation, concept, or theorem, etc., that is discussed in the manuscript. Consult the journal's Instructions for Authors for TOC graphic specifications.

A silicon-rhodamine chemical-genetic hybrid for far red voltage imaging from defined neurons in brain slice